International Journal of Automotive Technology, Vol. 6, No. 5, pp. 519–527 (2005)

1229-9138/2005/023-12

JOINING OF THIN-WALLED ALUMINUM TUBE BY ELECTROMAGNETIC FORMING (EMF)

Y.-B. PARK[1)*], H.-Y. KIM[2)] and S.-I. OH[1)]

[1)]School of Mechanical and Aerospace Engineering, Seoul National University, Seoul 151-742, Korea
[2)]Division of Mechanical and Mechatronics Engineering, Gangwon National University, Gangwon 200-701, Korea

(Received 5 February 2004; Revised 29 April 2004)

ABSTRACT–Recently, weight reduction of vehicles has been of great interest and consequently the use of low-density materials in the automotive industry is increasing every year. However, the substitution of one material for another is not simple because it accompanies several problems, for example, weakness in the strength and stiffness and difficulty in the joining. To overcome these problems, the structure of the automobile redesigned totoally. Aluminum spaceframe is rapidly being adopted as a body structure for accommodating lightness, stiffness and strength requirement. In aluminum spaceframe manufacturing, it is often required to join aluminum tube. However , there are few suitable methods for joining aluminum tube, so that much interest has been focused on testing suitable joining methods. Joining by electromagnetic forming (EMF) can be useful method in joining aluminum tube, which offers some advantages compared with the conventional joining methods. In this paper, joining by EMF was investigated as a pre-study for applying an automotive spaceframe. Finite element simulations and strength tests were performed to analyze the influence of geometric parameters on joint strength. Based on these results, configurations of axial joint and torque joint were suggested and guidelines for designing EMF joint were established.

KEY WORDS : Spaceframe, Electromagntic forming, Joint

1. INTRODUCTION

Vehicle weight reduction is one of the major methods for improving automotive fuel efficiency. The substitution of low-density materials such as aluminum, magnesium, plastics etc. for steel is a good example for vehicle weight reduction. Among lightweight materials, the use of high-strength aluminum alloy in the automotive industry is increasing every year. The substitution of one material for another is not simple because it accompanies several problems. Simple change of component material cannot achieve stiffness and strength, so that the automobile should be redesigned totally.

Spaceframe, or structural frame consisting of closed section members that can be extruded or hydroformed is rapidly becoming the chosen body structure for accommodating lightness, stiffness and strength requirements as an alternative to conventional monocoque (Kim *et al.*, 2002). Figure 1 shows a layout of an automotive spaceframe.

In aluminum spaceframe manufacturing, it is often required to join aluminum tube. But there are few suitable methods for joining aluminum tube, so that interest has been focused mainly on testing suitable joining methods. Resistance spot welding, which has been used for constructing conventional monocoque (Song *et al.*, 2004), has difficulties in joining aluminum tube. Several joining methods, instead of resistance spot welding, have been tried to construct automotive spaceframe. For instance, the Audi A2 spaceframe, which was evaluated for successful body design, was constructed via laser welding, metal insert gas (MIG) welding and self-piercing rivet (Barnes and Pashby, 2000).

Joining by EMF can be useful method in overcoming the limitations of conventional welding. Since there is no heat involved in the EMF process, significant problems associated with welding, for example distortion and weakening, are eliminated (Lianzhong *et al.*, 1993; Zhang *et al.*, 1995; Padmanabhan, 1997; Panshikar, 2000; Zhang *et al.*, 2001). Furthermore, EMF can be applied to join dissimilar materials, such as aluminum and steel. Low tooling cost and rapid joining time are other benefits of this process.

In this paper, joining by EMF was investigated as a pre-study for applying an automotive spaceframe. Finite element simulations and strength tests were performed to analyze the influence of geometric parameters of a

*Corresponding author. e-mail: pyb@plab2.snu.ac.kr

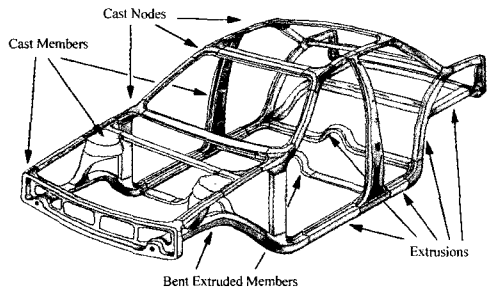

Figure 1. Layout of automotive spaceframe.

groove on joint strength. Based on these results, configurations of axial joint and torsion joint were suggested and guidelines for designing EMF joint were established.

2. FUNDAMENTALS OF ELECTROMAGNETIC FORMING

In EMF, a high current pulse is passed through a coil by the discharge of a capacitor bank. The current in the coil produces a transient primary magnetic field around the coil. The change in this field induces an eddy current in the workpiece and an associated secondary magnetic field. The two fields are repulsive and the force of magnetic repulsion causes the deformation of the workpiece. When the stress arising from repulsive magnetic pressure exceeds the yielding point of the workpiece material, plastic deformation of the workpiece begins (Lal *et al.*, 1968; Al *et al.*, 1974; Jablonski *et al.*, 1978). The resulting type of stress such as tensile or compressive stress depends on the type of coil used and the location of the workpiece relative to the coil. Tubular parts can be compressed or expanded by means of solenoid forming coils, whereas sheet metal can be formed by flat coils (Hashimoto *et al.*, 1993; Beley *et al.*, 1996; Beerwald *et al.*, 1999; Chunfeng *et al.*, 2002).

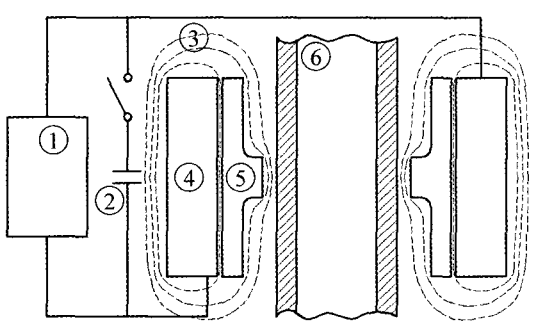

1 : Power supply 2 : Capacitor 3 : Magnetic flux lines
4 : Coils 5: Field shaper 6 : Tubular workpiece

Figure 2. Principle of an electromagnetic forming process.

Typical fields of application of such a forming process would be calibrating operations, as well as joining, embossing, or shearing operations. Among these applications, joining process is the most widely used operation today, either as an alternative but also supplementary to the conventional joining processes like welding, adhesive bonding or mechanical fastening. Figure 2 shows the principle of an electromagnetic compression process when a field shaper is used. As shown in the magnetic flux lines of Figure 2, a field shaper is used to concentrate the magnetic field where forming is needed.

3. DESIGN OF AXIAL JOINT

3.1. Experimental Procedure & Simulation Condition

Figure 3 illustrates a typical type to be used for joining by EMF. The joint force can be expressed as

$$F_{joing} = F_{friction} + F_{groove} \quad (1)$$

First term in equation (1) is the frictional force arising from contact pressure and last term is the restraining force caused by the groove. The frictional force is dependent on the frictional coefficient and the contact pressure. When an external force applied on the joint, the contact pressure becomes small or vanishes. So, the joint force supported by the frictional force become negligible during loading. Thus, the restraining force must be maximized to produce a strong joint. When a tensile load is exerted on this type of EMF joint, the joint will be separated from each other or failed (Hwang *et al.*, 1993; Lee *et al.*, 1994; Mahanian *et al.*, 1996; Murakoshi *et al.*, 1998). The occurrence of separation or failure of the joined tube can be determined by the rotation direction of

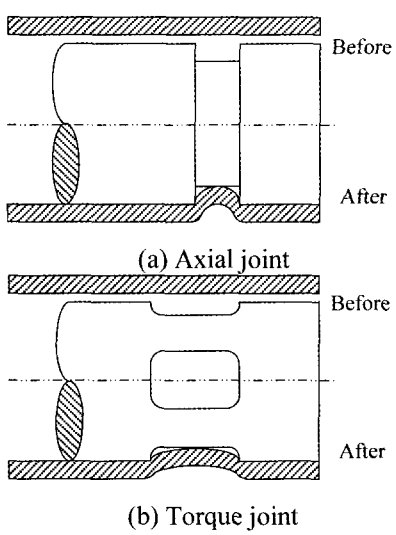

Figure 3. Typical type of EMF joint.

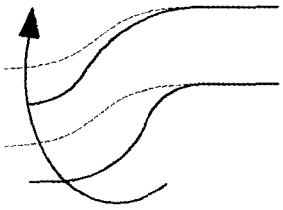

(a) Separation

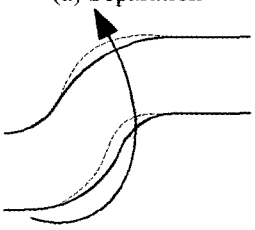

(b) Failure

Figure 4. Joint behavior on the groove profile according to the rotation direction.

the material on the groove profile. As shown in Figure 4, if the direction of this material is clockwise, joined tubes are separated from each other. If not, the tube will fail at the thinning point. In view of joint force or joint strength, it is better that the rotation of the material on the groove profile is counterclockwise rather than clockwise, i.e., inducing failure is better. But, just inducing failure is not optimal solution. Since the joint strength is closely related to the material thickness after compression forming, if thinning on the groove profile is large, inducing failure will be useless in view of joint strength. Therefore, both inducing failure and preventing thinning must be achieved simultaneously.

The rotation direction and the thinning magnitude can be determined by the geometry of the groove. Figure 5 shows the geometric design parameters of a groove, namely, groove radius, groove depth, groove width. In the following study, the influence of various design parameters on joint strength is analyzed by using finite element method and experiment.

A Maxwell Magneform machine with maximum charged energy of 16 kJ was used to perform electromagnetic compression. A universal compression coil with an inner diameter of 150 mm and height of 110 mm

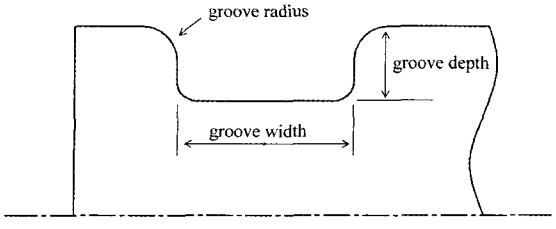

Figure 5. The geometric design parameters of the groove.

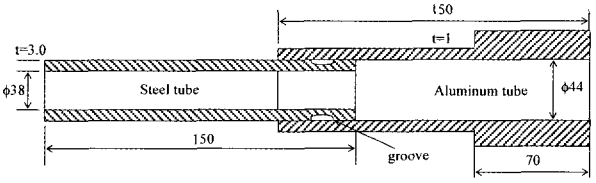

(a) Dimension of specimen

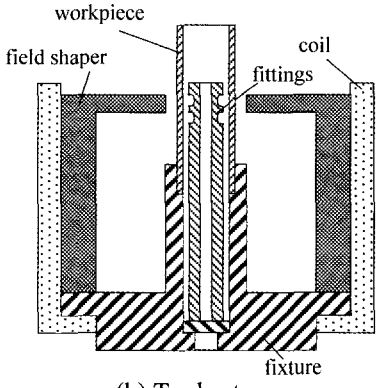

(b) Tool setup

Figure 6. Schematic view of experimatal equipement.

was used as the forming coil. The split cylindrical field shaper was made of Al 6061 and had a 50 mm outside diameter and 10 mm wall thickness. The inside protrusion part of the field shaper, which is used for concentrating magnetic pressure, had a diameter of 40 mm and a thickness of 10 mm. The deformation of aluminum tube is made by performing several magnetic pulse operations in the experiment by adjusting the location of the forming area. The experiment equipments are schematically shown in Figure 6(b). An Al 6063-T5 extruded tube was used as the workpiece material for the experiment. The workpiece has an outer diameter of 46 mm, wall thickness of 1mm, and axial length of 150 mm. The internal tube with the groove is made of high-strength steel. These specimens as shown in Figure 6(a) were used throughout this research. The groove was machined. Figure 7 shows the electromagnetic formed joints with a single groove used in strength test.

In finite element simulation, the workpiece was

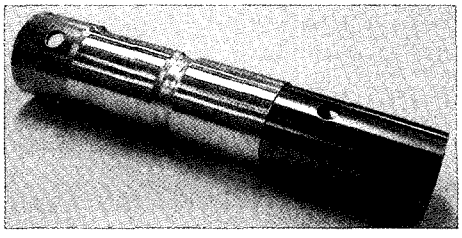

Figure 7. Electromagnetic formed joints with a single groove.

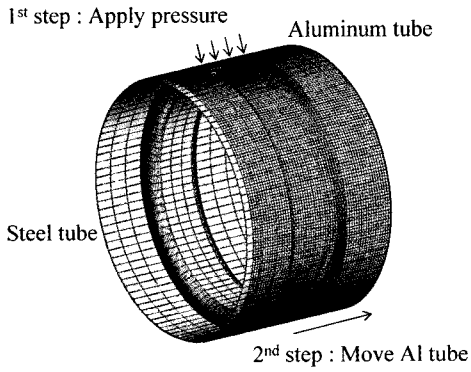

Figure 8. Finite element models and boundary condition.

considered as elasto-plastic material, and strain rate effects were neglected. The material properties of the workpiece are same as those of Al 6063-T6. The internal tube with the groove was considered as rigid body. The simulation was performed by two steps. First step is simulation of EMF for compressing aluminum tube and second step is simulation of tension test for pulling aluminum tube axially. In this study, finite element simulation was used for validating the tendency of the groove parameters on joint strength, not exact value. Figure 8 shows finite element models and boundary condition used in the simulation.

3.2. Influence of Design Parameters on Joint Strength

3.2.1. Effect of groove radius

Increasing the groove radius causes two opposite effects in terms of joint strength: Positive effect on joint strength is that thinning on the groove profile decreases after forming. Negative effect is that joined parts become easily separated because the rotation direction on the groove profile is clockwise. Thus, there exist an optimal groove radius at a given groove depth.

Figure 9 shows the normalized joint strength as a function of the groove radius at a fixed groove depth of 2 mm. The normalized joint strength is the predicted joint strength divided by the tensile strength of a material. There is a difference between finite element simulations and experiments. In simulations, the transition zone where failure turns to separation is between 0.5 mm and 0.7 mm. But in experiments, the transition zone is between 1.0 mm and 1.5 mm. This is due to the difference of contact location between simulations and experiments. The material on the groove corner does not contact with the groove corner entirely in experiment while contact is formed over the entire groove corner in simulations. This cause the difference of location of exerted force and consequently the difference of the rotation direction. Contact location in experiment is higher than finite element simulation, so that failure

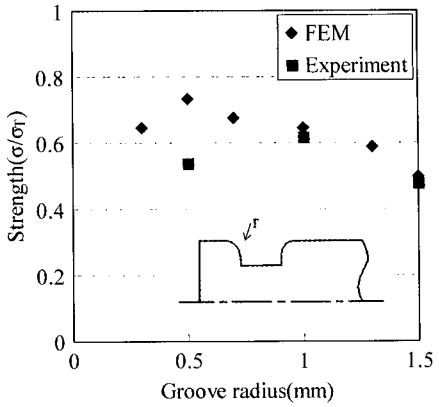

Figure 9. Effect of the groove radius on joint strength.

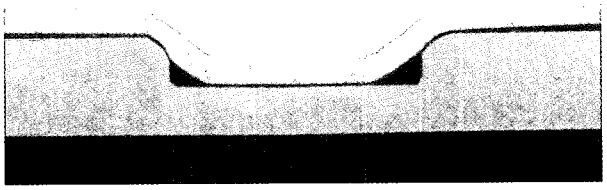

Figure 10. Cross sectional shape of electromagnetic formed joint in groove region.

behaviour tends to occurs in experiment. Figure 10 shows cross sectional shape of electromagnetic formed joint in groove region. As shown in Figure 9, it is seen that joint strength decrease at a larger groove radius than 1mm, i.e., separation occurs. It is inferred that optimal groove radius exist about 1 mm.

3.2.2. Effect of groove depth

Increasing the groove depth causes two opposite effects in terms of joint strength, as is the effect of the groove radius: Positive effect on joint strength is that the rotation

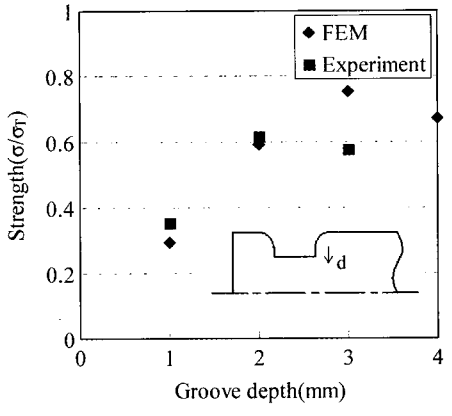

Figure 11. Effect of the groove depth on joint strength.

direction of the material on the groove profile is counter-clockwise because location of exerted force is high. Negative effect is that thinning is large and wrinkling may happen if tube is formed over compression limit ratio. Figure 11 shows the normalized joint strength as a function of the groove depth when the groove radius is fixed at 1 mm.

There is a difference between simulations and experiments. In simulations, the transition zone where separation turns to failure is between 2.0 mm and 3.0 mm. But in experiments, the transition zone is between 1.0 mm and 2.0 mm. As mentioned above, this is caused by the difference of contact location between simulations and experiments. Another reason is the difference of thickness after compression forming. As strain rate effect is neglected in finite element simulations, predicted thickness after applying pressure is different from real thickness. It is observed that thickness is overestimated in simulation. As shown in Figure 11, it is seen that joint strength decrease at a larger groove depth than 2 mm. It is inferred that optimal groove depth exist about 2 mm.

3.2.3. Effect of groove width

Increasing the groove width increases the contact area, which, in turn, increases the frictional force. In principal, frictional force have no concern with the contact area. But, in this case, since there exist residual hoop stress after compression formig, contact area can be considered as the area where hoop stress is exerted. Thus, increasing the groove width is thought to increase the frictional force. But this frictional force does not have a large effect on the joint strength because there is no movement in this area. Figure 12 shows the normalized joint strength as a function of the groove width when the groove radius and the groove depth are fixed to 1 mm and 2 mm, respectively. It is seen that there is little difference on joint strength over 10 mm of groove width.

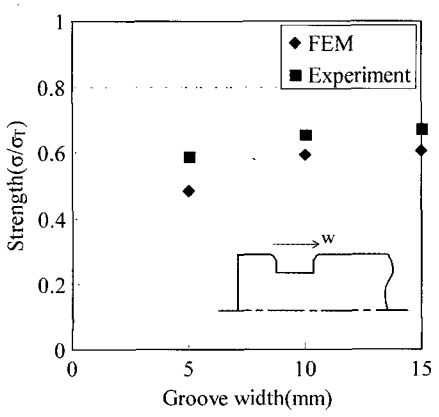

Figure 12. Effect of the groove width on joint strength.

3.2.4. Determination of groove parameters

So far, effect of various parameters on joint strength was studied. In this chapter, based on the above results, the value of these parameters is determined.

First, the groove width can be determined by the inflow of the material. For robust joining, the room for material inflow must be sufficient. From the results about the groove width, it can be concluded that the groove width should be 5–10 times material thickness, although it varies according to groove depth and groove radius. Second, the upper limit of the groove depth can be determined by compression limit ratio, which is known as about 5% in case of compressive forming of thin-walled tube (Min and Kim, 1993). But, in this type of forming, as tube is compressed partially, not totally, compression limit ratio is raised up to about 10% referring to experimental results. Thus, the upper limit of the groove depth can be set to 0.05D, where D is average diameter of the tube. The lower limit of the groove depth can be easily determined by material thickness. The minimum groove depth must be larger than material thickness for the room of material inflow. For the reason stated above, the range of the groove depth can be set between t and 0.05D. Third, the groove radius can be determined considering thickness change after compression forming. Considering previous experimental results and the groove geometry, it can be said that the groove radius should be larger than material thickness and smaller than about half of the groove depth.

Based on the above discussion, bounds of groove parameters in case of 1 mm material thickness and 45 mm average diameter can be express as

$$1 < d < 2.25,\ 1 < r < 1.125,\ w > 10 \qquad (2)$$

where d is the groove depth, r is the groove radius and w is the groove width.

With these bounds, the groove parameters can be easily determined: groove depth, groove radius and groove width can be set to 2 mm, 1 mm and 10 mm, respectively. However, it should be reminded that the groove dimensions and bounds is available only for single groove, not multiple grooves.

3.3. Suggestion of Axial Joint

There is a limit of joint strength when a single groove is used, even though the groove configuration is optimized. In other words, a single groove does not produce full strength of the material because thinning after EMF cannot be avoided. Thus, two or more grooves must be used to obtain full strength of the material. But, it is meaningless to increase two or more grooves with the same configuration because the joint strength is not made arithmetically. Combining two units of the groove which

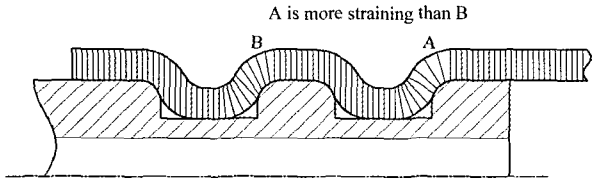

Figure 13. Schematic explanation of the differential strain.

have 50% joint strength does not yields 100% joint strength. This behaviour is due to stress concentration at the end of the tube caused by the differential strain of the outer member. Figure 13 shows schematic explanation of the differential strain. When a tensile load is exerted on joined tubes, the inner steel tube will move as a rigid body and the outer aluminum tube will suffer deformation. Each tube bears the full load just before the joint and transmits it gradually to the other. Thus the stress of outer Al tube will be highest at A and gradually diminish toward B. On the contrary the stress of the inner steel tube will be highest at B and diminish toward A. As the outer aluminum tube is extensible and the inner steel tube is inextensible, only the outer member will develop strains proportional to the existing stresses and failure will occur around A. In this paper, we shall count the groove from A to B. The first groove means the groove close to A.

Figure 14 shows the normalized joint strength of two combined grooves with various groove radii. It is seen that joints which have less thinning toward the first groove is stronger than the others. This is due to the stress concentration at the edge of the joint as mentioned above. Since the objective of this simulation is to validate the tendency of differential straining of the joined tube, experiment was omitted. To produce full strength of the

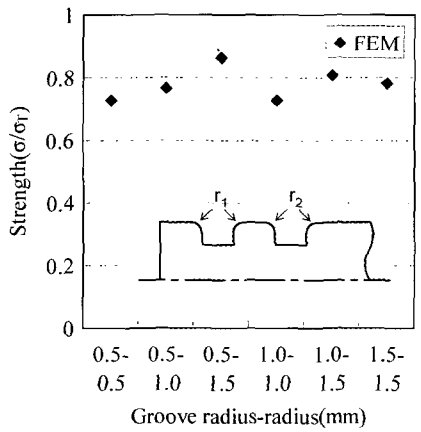

Figure 14. Effect of combination of two grooves on joint strength.

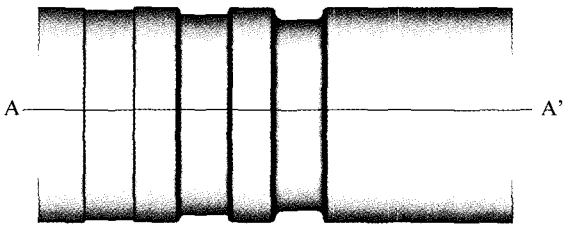

(a) Configuration of suggested axial joint.

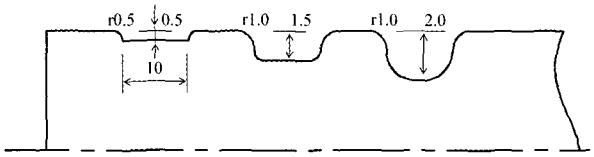

(b) A-A' section view

Figure 15. Suggested axial joint.

material, groove configuration can be determined as follows: first, material thickness on the first groove does not change because material thickness on the first groove directly determine joint strength. Second, the joint should be designed to reduce thinning toward the first groove, thus producing almost constant stress and strain throughout all grooves. For this, groove depth should be shallower and groove round be larger progressively toward the forst groove.

Figure 15 shows the configuration of suggested axial joint when a material thickness is 1mm. The dimension of each groove can be determined as follows: The dimension of the first groove was determined such that material thickness on the first groove does not change. But, with this dimension, the joint strength supported by the first groove is only about 30% of the full strength. The rest 70% strength should be supported by the other grooves. Two more grooves was combined to support the rest 70% strength and designed to reduce thinning toward the first groove. By several experiments and simulations, it was found that appropriate depth of the first and second groove is 75% and 25% of the third groove depth. Figure 16 shows the electromagnetic formed joint with suggestd groove dimensions. As a result of tension test, normalized joint strength reached only 88%. This is due to stress concentration at the tension test grip. Since

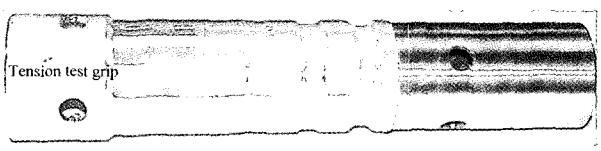

Figure 16. Electromagnetic formed joint with suggested groove dimensions.

failure occurred at the unformed section of the tube, it can be said that suggested axial joint has sufficient joint strength.

4. DESIGN OF TORQUE JOINT

4.1. Experimental procedure & Simulation condition

In a toque joint, the direction of load is circumferential. To resist the twisting force, a groove should be located in the axial direction. The techniques of designing torque joint are essentially the same with that of designing axial joint although there is a difference in geometric parameters. In designing a torque joint, the main geometric parameters are the number of grooves and the groove length in the axial direction. Basically, increasing the number of grooves or the groove length increases the resistance to torque. In general, the length of a joint zone is confined and the dimensions of a tube are given so that there is a limitation in increasing the values of these parameters.

EMF system and workpiece are the same as used in the previous test. The simulation was also performed by two steps. First step is simulation of EMF and second step is simulation of torsion test. But, torsion itself is complex and is greatly influenced by the specimen geometry and material anisotropy, so that computed torque may be not correct. In this paper, analysis of torque joint is limited to check deformed configuration.

4.2. Suggestion of Torque Joint

The groove of the torque joint can be designed by referring to the groove of an axial joint. The groove radius, the groove depth and the circumferential groove width can be set to 1 mm, 2 mm, 10 mm, respectively. Considering the circumference of the tube, the number of groove is set to six. The parameter only to determine is groove length in the axial direction. Minimum groove length to prevent separation of the joint was found by several finite element simulations and was set to 20 mm. Figure 17 shows simulation result of torsion test at 20 mm of groove length.

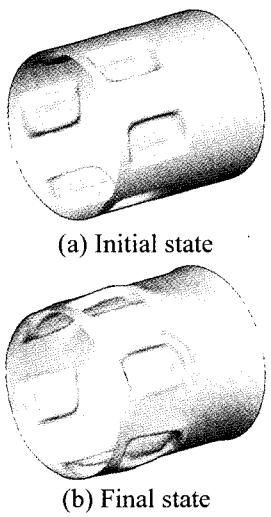

(a) Initial state

(b) Final state

Figure 17. Simulation result of torsion test at 20 mm of groove length.

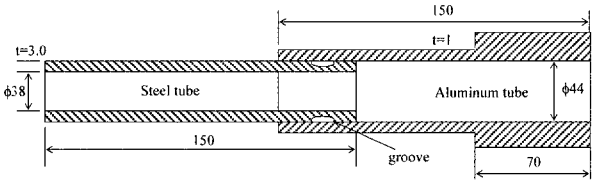

(a) Dimension of fixed-end joint

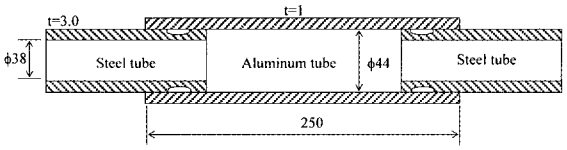

(b) Dimension of free-end joint

Figure 18. Specimen of torque joint.

Torsion tests were performed on two types of torque joints, fixed-end and free-end (Wu *et al.*, 1998). The shape and dimensions of each specimen are shown in Figure 18(a) and (b). The specimen of the fixed-end joint is similar to Lindholm-type specimen, which have been used by many investigators to conduct torsion tests. A very special feature of this specimen is that the gauge length is only a small fraction of the radius of the tube, so that a large shear strain can be achieved.

There is a considerable difference in deformed shape between these joints. In torsion test of the fixed-end joint, the buckling of the tube occurred as shown in Figure 19(a). The failure occurred at the shoulder part because of the stress concentration in this region. In torsion test of

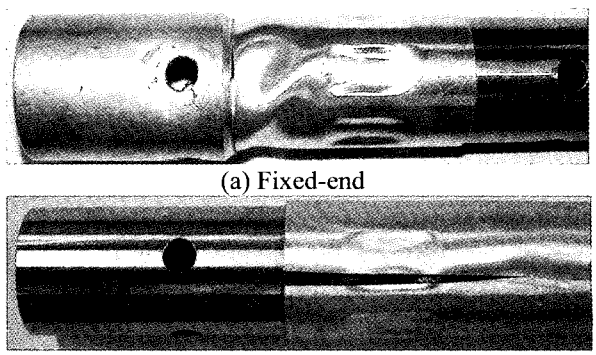

(a) Fixed-end

(b) Free-end

Figure 19. Deforemd shape of torque joint.

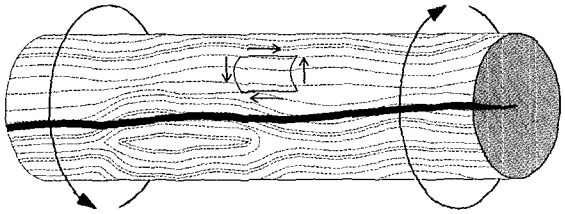

Figure 20. Stresses and failure pattern in wood.

the free-end joint, the failure occurred near the free end and in the axial direction, as shown in Figure 19(b). A possible explanation of this failure is found by torsion of the wood. Figure 20 shows stresses and failure pattern when the wood textured in the axial direction is twisted. When the tube is twisted, shear stresses occur in both circumferential and axial direction and consequently shear strain develop in both directions. In the material textured in the axial direction such as extruded aluminum tube and the wood, the shear resistance to the axial direction is smaller than the shear resistance to the circumferential direction due to material anisotropy, so that failure will develop in the axial direction. From the view of the joint strength, this type of failure is not good because it decrease the joint strength. Furthermore, since there is no work-hardening in this failure, weakness of the joint strength may even be greater. Figure 21 shows torque versus angle curve of these joints. It is seen that the joint strength of the fixed-end joint is larger than that of the free-end joint. It is also known that there is no work-hardening in the free-end joint.

As a result, to increase joint strength, the failure in the axial direction must be avoided and the failure in the circumferential direction must be induced. One of the methods for inducing failure in the circumferential direction is end-constraint like a shoulder of the fixed-end joint. The shoulder restricts the displacement in the axial direction, so that failure in the circumferential direction is induced. However, this method is difficult to apply because workpiece tube itself has to be machined. Another method is to combine groove of axial joint with groove of torque joint. If axial groove restrict the displacement in the axial direction, failure will occur in the circumferential direction. There may be various methods for adopting axial groove in the torque jont. Experiment about this method and study on the optimal torque joint are in progress.

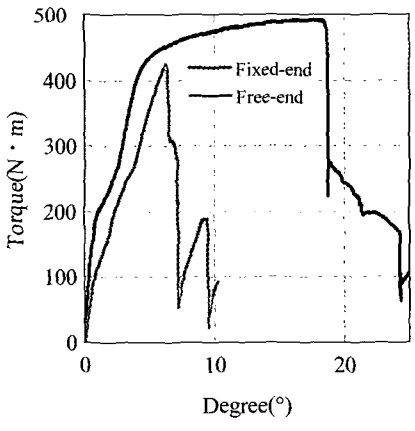

Figure 21. Torque vs. angle curve.

5. CONCLUSIONS

In the present paper, joining by EMF was investigated as a pre-study to the application of an automotive space-frame. Finite element simulations and experiments were performed to analyze the influence of geometric parameters of a groove on joint strength. Variation of joint strength with each geometric parameter was evaluated. Based on these results, the following conclusions can be drawn:

(1) Axial joint should be designed such that material thickness on the first groove which is close to loading does not change and thinning after compression forming is reduced toward the first groove.
(2) Suggested axial joint showed 88% of joint strength. This is due to stress concentration at the tension test grip. Since failure occurred at the unformed section of the tube, it can be said that suggested axial joint has sufficient joint strength.
(3) Torsion tests were performed on two types of torque joint, fixed-end and free-end joint. The joint strength of the fixed-end joint is larger than that of the free-end joint.
(4) Torque joint should be designed such that axial displacement during torsion is suppressed.

ACKNOWLEDGEMENT–The authors would like to acknowledge Next Generation Vehicle Technology (NGV) and Hyundai Motor Company (HMC) for supporting this study.

REFERENCES

Al-Hassani, S. T. S., Duncan, J. L. and Johnson, W. (1974). On the parameters of the magnetic forming process. *Journal Mechanical Engineering Science,* **16**, 1–9.

Barnes, T. A. and Pashby, I. R. (2000). Joining techniques for aluminum spaceframe used in automobiles Part I – solid and liquid phase welding. *J. Materials Processing Technology,* **99**, 62–71.

Barnes, T. A. and Pashby, I. R. (2000). Joining techniques for aluminum spaceframe used in automobiles Part II –

adhesive bonding and mechanical fasteners. *J. Materials Processing Technology,* **99**, 72–79.

Beerwald, C., Brosius, A., Homberg, W., Kleiner, M. and Wellendorf, A. (1999). New aspects of electromagnetic forming. Advanced Technology of Plasticity. *Proc. of the 6th ICTP* **3**, 2471–2476.

Beley, I. V., Ferrtik, S. M. and Khimenko, L. T. (1996). *Electromagnetic forming handbook.* English Version of Russian book translated by M. M. Altynova, Ohio State University.

Chunfeng, L., Zhiheng, Z., Jianhui, L., Yongzhi, W. and Yuying, Y. (2002). Numerical simulation of the magnetic pressure in tube electromagnetic bulging. *J. Materials Processing Technology,* **123**, 225–228.

Hashimoto, N., Wang, X. and Negishi, H. (1993). Electromagnetic forming of thin-walled metal tube with fine grooves, Advanced Technology of plasticity. *Proc. the Fourth International Conference on Technology of Plasticity,* 533–538.

Kim, H. Y., Kim, J. K., Heo, S. J. and Kang, H. (2002). Design of the impact energy absorbing members and evaluation of the crashworthiness for aluminum intensive vehicle. *Trans. Korean Society of Automotive Engineers* **10**, **1**, 216–233.

Hwang, W. S., Lee, J. S., Kim, N. H. and Sohn, H. S. (1993). Joining of copper tube to polyurethane tube by electromagnetic pulse forming. *J. Materials Processing Technology,* **37**, 83–93.

Jablonski, J. and Winkler, R. (1978). Analysis of the electromagnetic forming process. *Int. J. Mech. Sci.,* **20**, 315–325.

Lal, G. K. and Hillier, M. J. (1968). The electrodynamics of electromagnetic forming. *Int. J. Mech. Sci.,* **10**, 491–500.

Lee, S. H. and Lee, D. N. (1994). Finite element analysis for electromagnetic forming for tube compression, Trans. of ASME. *J. Engineering Material and Technology* **116**, **2**.

Lianzhong, Y., Bingqin, Z., Shihong, Z. and Haizhi, X. (1993). The deformation and strain distribution of metal frame parts in electromagnetic forming, Advanced Technology of Plasticity. *Proc. the 4th ICTP* 1867–1870.

Mahanian, S. and Blackwell, D. B. (1996). Finite element analysis of electromagnetic forming of tubes with fittings. *MED-Manufacturing Science and Engineering,* **4**, 323–329.

Min, D. K. and Kim, D. W. (1993). Finite element analysis of the electromagnetic tube-compression process. *J. Materials Processing Technology* **38**, **1–2**, 29–40.

Murakoshi, Y., Takahashi, M., Sano, T., Hanada, K. and Negishi, H. (1998). Inside bead forming of aluminum tube by electo-magnetic forming. *J. Materials Processing Technology* **80–81**, 695–699.

Padmanabhan, M. (1997). *Wrinkling and Springback in Electromagnetic Sheet Metal Forming and Electro-Magnetic Ring Compression*, Ph.D. Dissertation, Ohio State University.

Panshikar, H. M. (2000). *Electromagnetic Forming and Impact Welding*, Ph.D. Dissertation, Ohio State University.

Song, J. H., Noh, H. G., Akira, S. M., Yu, H. S., Kang, H. Y. and Yang, S. M. (2004). Analysis of effective nugget size by infrared thermography in spot weldment. *Int. J. Automotive Engineers* **5**, **1**, 55–59.

Wu, Han-Chin, Xu, Zhiyou and Wand, Paul T. (1998). Torsion test of aluminum in the large strain range. *J. Material Plasticity* **13**, **10**, 873–892.

Zhang, H., Murata, M. and Suzuki, H. (1995). Effects of various working conditions on tube bulging by electromagnetic forming. *J. Materials Processing Technology,* **48**, 113–121.

Zhang, S. B. and Neghishi, H. (2001). Curling of square tube by electromagnetic forming. *Impact Engineering and Application,* 285–290.